

# SINGLE TRANSIENT K CHANNELS IN MAMMALIAN SENSORY NEURONS

H. KASAI\*, M. KAMEYAMA†, K. YAMAGUCHI†, AND J. FUKUDA\*

\**Department of Physiology, Faculty of Medicine, University of Tokyo, Bunkyo-ku, Tokyo 113, Japan;*

*and †National Institute for Physiological Sciences, Myodaiji-cho, Okazaki 444, Japan*

**ABSTRACT** A single-channel recording of the transient outward current (A-current) was obtained from dorsal root ganglion cells in culture using patch-clamp techniques. Depolarization of the membrane patch elicited pulse like current of a uniform amplitude in an outward direction, of which the unitary conductance was 20 pS. Alteration of extracellular ionic compositions indicated that the charge carriers were K ions. A systematic study was made on the voltage-dependence of the ensemble average current; (a) the activation started at a potential around  $-60$  mV; (b) the time course of the activation was relatively rapid; (c) the channel was completely inactivated at a potential positive to  $-40$  mV. Two time constants ( $\tau_f = 100$  ms and  $\tau_s = 4,000$  ms) were detected in the decay of the current indicating that the channels had two different states of inactivation. A convulsant, 4-aminopyridine (4-AP), acted on the channel only from the intracellular side of the membrane. 4-AP (5 mM) reduced not only mean open time (by 50%) but also the single-channel conductance (by 20%). The properties of the channel were independent of Ca ions in the intracellular space.

## INTRODUCTION

Mammalian neuronal membranes display four K currents (1, 2): (a) the delayed K current first described in the squid giant axon (3), (b) a transient outward current (A-current) (4, 5), (c) a Ca-activated K current (6) and (d) the *M*-current (7). The latter three K currents are thought to be important in modulating synaptic potentials (7–11), building spike-encoding properties (12–14), and suppressing neuronal Ca influx (15). The separation of each current is difficult with conventional voltage-clamp techniques, firstly, because all of these currents are activated by membrane depolarization and are transported by the same ionic species (K ions), and, secondly, because there is no specific blocker for each type of K channel. The patch-clamp technique (16), though, provides a method for examining these currents because it can isolate single channel currents. Indeed, this technique has clarified fine features of ion channels carrying delayed K current (17) and Ca-activated K current (18).

We have employed the patch-clamp technique to study the A-current at the single-channel level in cultured dorsal root ganglion cells. We report here that the A-current is carried through a specific type of K channel having a conductance of 20 pS. The channel can be activated from a potential close to the resting membrane potential ( $-60$  mV), and it is completely inactivated at potentials positive to  $-40$  mV. The inactivation consists of an initial fast

process ( $\tau_f = 100$  ms) followed by a very slow process ( $\tau_s = 4$  s). The convulsant 4-aminopyridine (19) suppresses the A-current by reducing both the conductance and opening probability of the single-channels. These properties provide a new basis for understanding the roles of the A-current in neurons and in neuronal networks.

## METHODS

The patch-clamp technique (16) was applied to dorsal root ganglion cells from adult guinea pigs (20) grown on poly-L-lysine coated plastic dishes (35 mm Lux, U.S.A.) in a serum free culture medium, which contained DMEM ( $\frac{1}{2}$  volume), Ham's F12 ( $\frac{1}{2}$  volume), insulin (5  $\mu$ g/ml), transferrin (30  $\mu$ g/ml), putrescine (100  $\mu$ M), progesterone (100  $\mu$ M), and selenite (30 nM) (21). The nerve cells were bathed in a high-K solution (150 mM KCl, 1 mM MgCl<sub>2</sub>, 1 mM EGTA, 5 mM Na-Hepes, 5.5 mM glucose at pH 7.4, 20–24°C) during the patch-clamp experiments. The resting potential of the cell membrane was assumed to be 0 mV. Patch electrodes (6–12 mega  $\Omega$ ) were filled with a Na-free solution (150 mM Tris-HCl, 5 mM KCl, 1 mM CaCl<sub>2</sub>, and 1 mM MgCl<sub>2</sub>, at pH 7.4). Current signals were filtered with a cut-off frequency of 1 kHz and stored on FM magnetic tapes. Capacitive transient currents and leakage currents were compensated by the conventional technique: (a) reducing them by the aid of an analogue circuit (16) during experiments and (b) subtracting a current trace without channel openings using a digital computer.

At least five types of single-channel currents were found: the A-current (20 pS), two types of delayed K currents (7 pS and 50 pS) and two types of Ca-activated K currents (70 pS and 200 pS). We selected those patches in which only the A-current channels were present. Currents other than A-current were easily detected because the A-current was completely eliminated by sustained depolarization (for 30 s to 0 mV).

We used cell-attached patches unless otherwise noted (51 cell-attached, 30 inside-out, and 5 outside-out patches). The effects of 4-aminopyridine (4-AP) were studied using 5 cell-attached, 22 inside-out, and 5 outside-out patches. The 4-AP solutions were made by adding

All correspondence should be sent to Dr. H. Kasai, Department of Physiology, Faculty of Medicine, University of Tokyo, Bunkyo-ku, Tokyo 113, Japan.

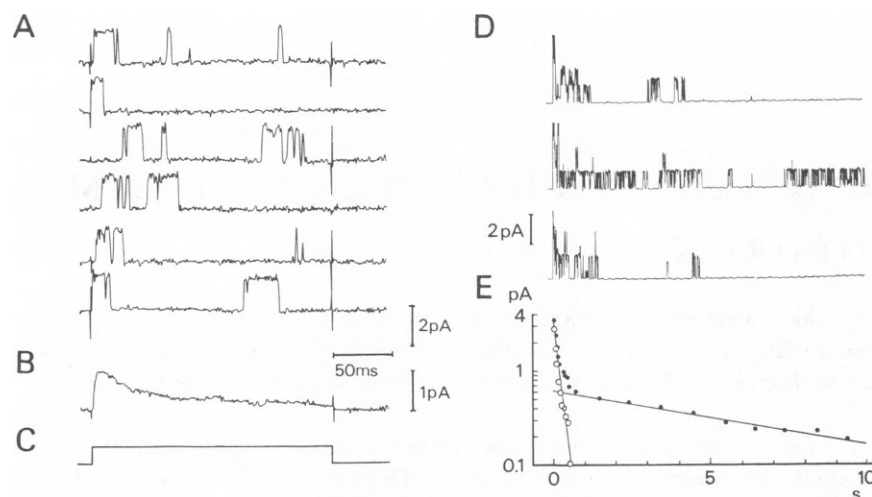


FIGURE 1 Single A-currents recorded from membrane patches of cultured mammalian neurons. (A–C) single A-current (A) was elicited by depolarization from  $-100$  mV to  $-10$  mV (C). The depolarization was applied every 4 s; outward current is represented by an upward deflection. An ensemble average current (B) was calculated from 135 current records. (D) single-channel currents elicited by a 10 s depolarization command from  $-90$  mV to  $0$  mV. The depolarization was applied every 30 sec. This patch exhibited 4 simultaneous openings. (E) a semilogarithmic plot of the ensemble average current (filled circles) revealing two time constants in the inactivation. The ensemble average current was obtained as follows: (a) the command period was divided into consecutive intervals (a duration of the interval was either 50 ms until 500 ms after the onset of depolarization or 1 s from 500 ms to 9.5 s, respectively); (b) amplitude of A-currents averaged during an interval was obtained for each current trace; (c) the ensemble average current during the interval was calculated from 32 traces. The two time constants were 8 s ( $\tau_s$ ) and 120 ms ( $\tau_f$ ), in this particular patch. Open circles give current remaining after removing the slow exponential component.

4-AP to either the normal pipette solution or the high-K bathing solution and the pH was readjusted to 7.4.

## RESULTS

Fig. 1 A shows a single A-current elicited by a depolarization of the patch from a holding potential of  $-100$  mV to  $-10$  mV. A 1.5 pA outward current frequently appeared soon after the onset of the depolarization. An ensemble average in Fig. 1 B illustrates that the current was maximal approximately 8 ms after the depolarization. The inactivation was gradual; the current persisted 200 ms after the depolarization. The entire time course of the inactivation was examined with a depolarization lasting for 10 s (Fig. 1 D). A model consisting of the sum of two underlying exponential processes, with time constants of 100 ms ( $\tau_f$ , fast inactivation) and 4 s ( $\tau_s$ , slow inactivation), fits the ensemble average current data (Fig. 1 E), and indicates that there are two inactivated states.

The  $I$ - $V$  plot for the amplitude of a single A-current was linear at membrane potentials between  $-50$  mV and  $50$  mV (Fig. 2). The single channel conductance was calculated to be  $20.1 \pm 3.7$  pS (means  $\pm$  SD,  $n = 15$ ). The major charge carrier through the channel was determined to be K<sup>+</sup> ions from the observation that a 10-fold increase in [K<sup>+</sup>] shifted the reversal potential of the current by 52 mV in a depolarizing direction (Fig. 2).

The voltage-dependence of a single A-current was studied by analysing ensemble average currents at different test depolarizations (Fig. 3 A). Fig. 3 B shows the relationship between the test depolarization and the normalized

value of the peak current (see Fig. 3 legend). A 50% activation of the channel was reached at  $-30$  mV, and 90% activation was attained at  $0$  mV. Note that the activation of the channel starts at around  $-60$  mV, which suggests that the channel can be activated even by a small depolarization at the resting membrane potential level of the dorsal root ganglion cell ( $-50$  to  $-70$  mV [22]). Time

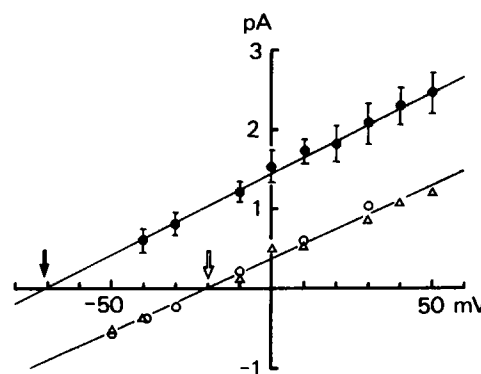


FIGURE 2 Amplitude of single A-currents (ordinate) plotted against membrane potential of patches (abscissa). Filled circles were obtained from an electrode containing 5 mM K<sup>+</sup>; each point was the average of 5–15 patches. Bars represent S.D. A linear regression line gave the mean conductance of the channel, 20.1 pS. The extrapolated reversal potential was  $-71$  mV (filled arrow). Open symbols were obtained from an electrode containing 50 mM K<sup>+</sup> (solution in the pipette was 105 mM NaCl, 50 mM KCl, 1 mM CaCl<sub>2</sub>, 1 mM MgCl<sub>2</sub>, 5 mM Na-Hepes); the circles and triangles represent data taken from two different patches. The reversal potential was shifted to  $-19$  mV (open arrow).

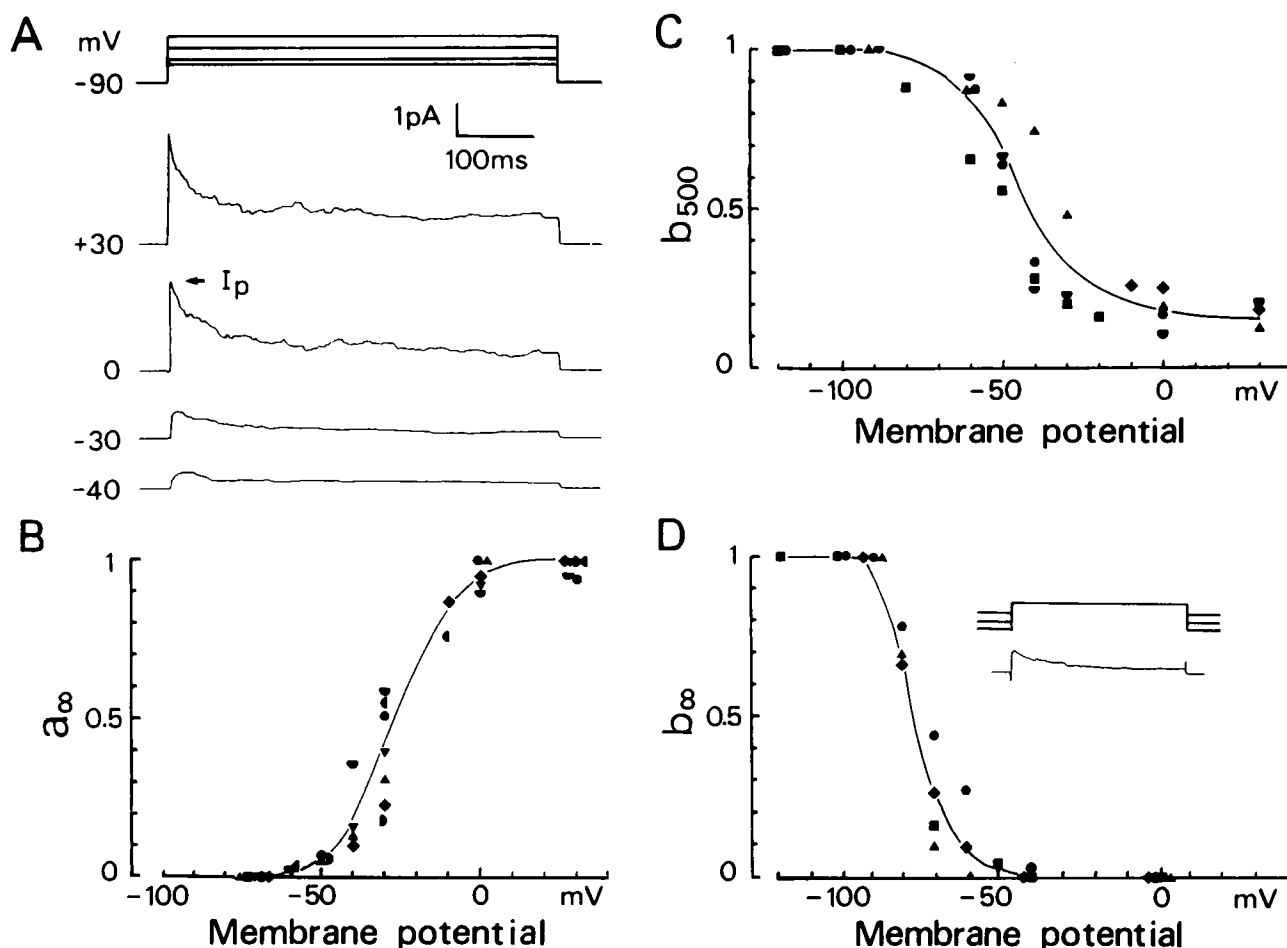


FIGURE 3 Voltage-dependence of the activation and inactivation of A-current studied by ensemble average currents. (A) ensemble average currents elicited by depolarization of a membrane patch from  $-90$  mV to various test potential levels (indicated in the figure). (B) normalized values of the peak current amplitude ( $a_8(V)$ , ordinate) plotted against the test potential ( $V$ , abscissa);  $a_8(V)$  were obtained from the equation:  $I_p(V)/i(V) = (I_p(30)/i(30)) \cdot a_8(V)$ , where  $I_p(V)$  was the peak amplitude of the current,  $i(V)$  was the amplitude of a single-channel current, and  $I_p(30)$  and  $i(30)$  were values of  $I_p(V)$  and  $i(V)$ , respectively at the test potential of  $+30$  mV. C and D illustrate voltage-dependence of the inactivation induced by the fast and slow processes, respectively. (c) normalized amplitude of current at 500 ms after the onset of depolarization ( $b_{500}(V)$ , ordinate) plotted against the test potential ( $V$ , abscissa). The value of  $b_{500}(V)$  was obtained by  $I_{500}(V) = I_p(V) \cdot b_{500}(V)$ , where  $I_{500}(V)$  was amplitude of current 500 ms after the depolarization, and  $I_p(V)$  was peak amplitude. (D) the steady-state inactivation. In this experiment, the membrane potential of the patch was depolarized to a constant level ( $0$  mV), while the holding potential was varied (inset). Normalized values ( $b_8(V)$ , ordinate) of the peak amplitude were plotted against various holding potential levels ( $V$ , abscissa). The value of  $b_8(V)$  was obtained by  $I_p(V) = I_p(-100) \cdot b_8(V)$ , where  $I_p(V)$  was the peak amplitude of the current elicited by depolarization to  $0$  mV from holding potential ( $V$ ), and  $I_p(-100)$  was  $I_p(V)$  at the holding potential of  $-100$  mV. Solid lines in B–D were drawn by eye. Same symbol represents data taken from the same patch.

to peak of average currents was smaller at larger membrane depolarization; smaller than 4 ms at 30 mV, 8 ms at 0 mV, and 19 ms at  $-30$  mV ( $n = 4$ ).

The two inactivation processes shown in Fig. 1 E (fast and slow inactivation) have different voltage-dependent behaviors (Fig. 3 C and D). Fig. 3 C illustrates the voltage-dependence of the inactivation that chiefly represented the fast inactivation; i.e., normalized values of the current at 500 ms after the onset of the depolarization ( $b_{500}(V)$ ) were plotted against the test potential ( $V$ ). Even at  $+30$  mV, the maximum inactivation attained by the fast process ( $b_{500}(V)$ ) was 80%. This can be contrasted with the behavior of the slow process by comparing Fig. 3 C and D. Fig. 3 D

illustrates the voltage-dependence of the inactivation attained both by the fast and slow inactivation processes; i.e., membrane potentials of patches were depolarized to a constant potential ( $0$  mV) from different holding levels and normalized peak amplitude values ( $b_8(V)$ ) were obtained as a function of the holding potential ( $V$ ). Comparison of the two inactivation curves (Fig. 3 C and D) indicates that the slow process ( $b_8 \neq b_{500}/b_f$ ) has a steeper voltage-dependence than the fast process at the resting membrane potential. Another difference is that the slow process inactivates the channel almost completely at  $-40$  mV. The time constant of the fast inactivation process ( $\tau_f$ ) was voltage-dependent (the time constants were estimated

using logarithmic plots as shown in Fig. 1 *D*);  $180 \pm 80$  ms at  $-30$  mV,  $100 \pm 40$  ms at  $0$  mV and  $60 \pm 30$  ms at  $30$  mV (mean  $\pm$  SD,  $n = 7$ ). By contrast, the time constant of the slow inactivation ( $\tau_s$ ) was  $4.3 \pm 2.5$  s ( $n = 4$ ) and was less dependent on membrane potential between  $-50$  mV and  $30$  mV.

The kinetics of the single channel was independent of Ca ions in the intracellular space; (a) no change in the kinetics was detected when the membrane patch was excised from the cell (the inside-out patch configuration), nor when the Ca concentration in the intracellular side of the membrane was increased, in sequence, from below  $10^{-8}$  M (10 mM EGTA),  $10^{-6}$  M (0.93 mM Ca and 1 mM EGTA), to  $10^{-5}$  M (three experiments); (b) the single-channel currents recorded by the pipette filled with a Ca-free solution (1 mM EGTA) had the same properties (three experiments) as the currents recorded by the pipette filled with the normal pipette solution containing 1 mM Ca ions. (This negated the possibility that the kinetics were regulated by extracellular Ca ions which flew through the patch-membrane into the intracellular space during the depolarization.) However, when the patch-pipette containing 3 mM Co ions (3 mM  $\text{CoCl}_2$  was added to the normal pipette solution) was used, the time course of the activation was slowed, and the voltage-dependence of the kinetics appeared to be shifted in the depolarizing direction by  $\sim 10$  mV. This may be attributed to the stabilizing effect of the divalent cations.

4-aminopyridine had two effects on the single-channel current when it was applied from the intracellular side of the membrane using the inside-out patch configuration. First, 4-AP reduced the single-channel conductance in a dose-dependent manner. In the representative records in Fig. 4, 5 mM 4-AP reduced the amplitude of the single channel current by 20%, while the reversal potential was not shifted (data not shown). A 50% reduction in the conductance was reached at 12 mM ( $K_{D,p}$ : mean,  $n = 4$ ). Second, 4-AP reduced the opening probability of the channel; the mean open time was reduced, and the mean closed time was prolonged (see Fig. 4 *B*). Accordingly, the ensemble average current was reduced in amplitude (Fig. 4 *D*). A 50% reduction in the peak amplitude of the ensemble average current was reached at 1 mM 4-AP ( $K_{D,p}$ : mean,  $n = 4$ ). The  $K_{D,p}$  was more than ten times smaller than the  $K_{D,r}$ , which indicates that the suppression of the K current was mainly due to the change in the open-close kinetics. Both effects of 4-AP were reversible (Fig. 4 *C*).

4-AP acted on the single-channel only from the intracellular side of the membrane; (a) the single-channel currents recorded by the pipette containing 5 mM 4-AP had the same kinetics as recorded by the pipette containing the normal solution (4 experiments); (b) when 4-AP (up to 5 mM) was applied from the extracellular side of the membrane using the outside-out patch configuration, neither the conductance nor the kinetics was affected by 4-AP

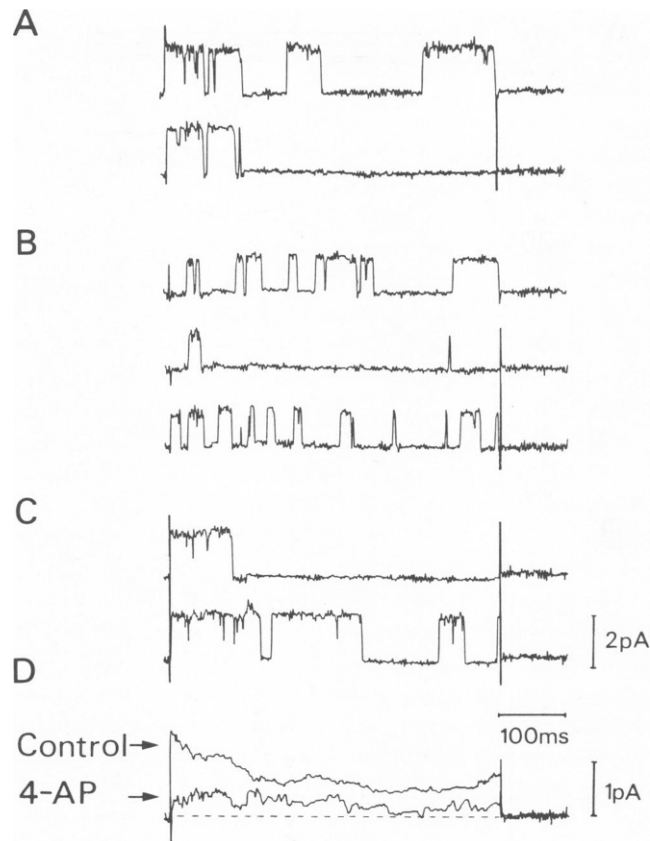


FIGURE 4 Effects of 4-aminopyridine on the single A-current. Currents were recorded from an inside-out patch in which intracellular side of the membrane was exposed to the bathing solution and was continuously perfused. (A) in the control solution, (B) in the presence of 5 mM 4-AP, and (C) after removal of 4-AP, respectively. The patch was depolarized from  $-100$  mV to  $0$  mV. 4-AP reduced the amplitude of the single-channel current (from  $1.8$  pA to  $1.4$  pA), which was associated with change in the kinetics. The mean open time was reduced (from  $15$  ms to  $8$  ms), and the mean closed time was increased (from  $4$  ms to  $15$  ms). (D) 4-AP reduced the ensemble average currents. The average currents (superposed) were calculated from 25 current records in control, and 33 in 4-AP.

(five experiments). When 4-AP was applied to the bathing solution during the cell-attached patch recording, the effects were the same as when applied intracellularly, the only exception being that the 4-AP effects appeared very slowly; taking 1 to 2 min to reach the steady-state level, and more than 3 min to be eliminated after the removal of 4-AP (six experiments). These data indicate that the 4-AP molecules, applied extracellularly, can permeate the plasma membrane slowly, and act on the K-channel from the intracellular side of the membrane.

## DISCUSSION

The present patch-clamp study has revealed several new properties of the A-current. First, the A-current is carried through a specific type of channel (A-channel) whose conductance is  $20$  pS. Second, the channel can be opened at the resting membrane potential level ( $-60$  mV). Third,

the channel is inactivated by depolarization with two  $\tau$ 's, 100 ms ( $\tau_f$ ) and 4 s ( $\tau_s$ ) at 0 mV. Fourth, the slow inactivation process ( $\tau_s$ ) completely inactivates the channel at potentials positive to -40 mV. Fifth, intracellular Ca ions are not necessary for either activation or inactivation of the channel. Finally, 4-AP reduces both the conductance and the opening probability of the channel.

The A-current has been considered to play important roles in forming low frequency repetitive spike discharges (12–14) and building central delay into neuronal networks (9). The involvement of the A-current in these phenomena is plausible in light of the two properties confirmed in this study: first, the A-current can be activated from a small depolarization level so that the A-current is able to suppress spike generation, and second, the A-current has strong inactivation kinetics, such that spike initiation is delayed from the onset of depolarization until the A-current is inactivated.

Recently, the A-current has been reported to be essential in forming very long central delays (3 s) which are important in the inking-behaviour of *Aplysia* (10). This is based on the observation that the delay is removed suppressing the A-current either by 4-AP application or conditioning depolarization. A similar 4-AP sensitive long central delay (up to 750 ms) has been reported in mammalian brain-stem neurons which is related to respiratory rhythm generation (11). These long delays are difficult to explain in light of the fast inactivation of the A-current ( $\tau$  is about 100 ms). The slow inactivation which we confirmed in this paper may provide a basis for understanding the long delays. The slow inactivation process of the A-current has been difficult to confirm with conventional voltage clamp techniques because other voltage-dependent K currents can be co-activated during the depolarization. However, studies using other preparations (guinea pig hippocampal pyramidal cells [1], frog nodes of Ranvier [23], and locust muscle [24]), have noted a slowly decaying current component associated with the A-current. Hence, the A-current may play a role in introducing long delays which are critical in the programming of animal behaviour in different neuronal circuits.

We thank Dr. C. D. Balaban and Dr. Y. Kurachi for reading the manuscript.

This study was supported by grants 58060001 and 59123004 from the Japanese Ministry of Education, Science and Culture.

Received for publication 16 July 1985 and in final form 27 December 1985.

## REFERENCES

1. Gstaßson, B., M. Galvan, P. Grafe, and H. Wigstrom. 1982. A transient outward current in a mammalian central neurone blocked by 4-aminopyridine. *Nature (Lond.)* 299:252–254.
2. Galvan, M., and C. Sedlmer. 1984. Outward currents in voltage-clamped rat sympathetic neurones. *J. Physiol. (Lond.)* 356:115–133.
3. Hodgkin, A. L., and A. F. Huxley. 1952. A quantitative description of membrane current and its application to conduction and excitation in nerve. *J. Physiol. (Lond.)* 117:500–544.
4. Connor, J. A., and C. F. Stevens. 1971. Voltage clamp studies of a transient outward membrane current in gastropod neuronal somata. *J. Physiol. (Lond.)* 213:21–31.
5. Neher, E. 1971. Two fast transient current components during voltage clamp on snail neurones. *J. Gen. Physiol.* 58:36–53.
6. Krnjevic, K., E. Puil, and R. Werman. 1978. EGTA and motoneuronal after potentials. *J. Physiol. (Lond.)* 275:199–223.
7. Adams, P. R., D. Brown, and J. F. Halliwell. 1981. Cholinergic regulation of M-current in hippocampal pyramidal cells. *J. Physiol. (Lond.)* 317:29P.
8. Shimahara, T. 1983. Presynaptic modulation of transmitter release by the early outward potassium current in *Aplysia*. *Br. Res.* 263:15–16.
9. Daut, J. 1973. Modulation of the excitatory synaptic response by fast transient K<sup>+</sup> current in snail neurones. *Nature New Biol.* 246:193–196.
10. Byne, J. H., E. Shapiro, N. Dineringer, and J. Koster. 1979. Biophysical mechanisms contributing to inking behavior in *Aplysia*. *J. Neurophysiol.* 42:1233–1250.
11. Dekin, M. S., and P. A. Gettings. 1984. Firing pattern of neurons in the nucleus tractus solitarius: modulation by membrane hyperpolarization. *Brain Res.* 324:180–184.
12. Connor, J. A., and C. F. Stevens. 1971. Prediction of repetitive firing behaviour from voltage clamp data on an isolated neurone soma. *J. Physiol. (Lond.)* 213:31–53.
13. Connor, J. A. 1975. Neural repetitive firing: a comparative study of membrane properties of crustacean walking leg axons. *J. Neurophysiol.* 38:922–932.
14. Connor, J. A. 1978. Slow repetitive activity from fast conductance changes in neurons. *Fed. Proc.* 37:2139–2145.
15. Llinas, R., and M. Sugimori. 1980. Electrophysiological properties of in vitro Purkinje cell dendrites in mammalian cerebellar slices. *J. Physiol. (Lond.)* 305:197–213.
16. Hamill, O. P., A. Marty, E. Neher, B. Sakmann, and F. J. Sigworth. 1981. Improved patch-clamp techniques for high-resolution current recording from cells and cell-free membrane patches. *Pflügers Arch. Eur. J. Physiol.* 391:85–100.
17. Conti, F., and E. Neher. 1980. Single channel recordings of K currents in squid axons. *Nature (Lond.)* 285:140–143.
18. Marty, A. 1981. Ca-dependent K channels with large unitary conductance in chromaffin cell membrane. *Nature (Lond.)* 291:497–500.
19. Thompson, S. J. 1977. Three pharmacologically distinct potassium channels in molluscan neurones. *J. Physiol. (Lond.)* 265:465–488.
20. Fukuda, J., and M. Kameyama. 1979. Enhancement of Ca spikes in nerve cells of adult mammals during neurite growth in tissue culture. *Nature (Lond.)* 279:546–548.
21. Yamaguchi, K. 1983. Selective reduction of Ca spikes in nerve cell cultured in an a serum-free medium. *J. Physiol. Soc. Jpn.* 45:403.
22. Sato, M., and G. Austin. 1961. Intracellular potentials of mammalian dorsal root ganglion cells. *J. Neurophysiol.* (Bethesda) 24:569–582.
23. Dubois, J. M. 1981. Evidence for the existence of three types of potassium channels in the frog ranvier node membrane. *J. Physiol. (Lond.)* 318:297–316.
24. Salkoff, L., and R. Wyman. 1980. Facilitation of membrane electrical excitability in *Drosophila*. *Proc. Natl. Acad. Sci. USA.* 77:6216–6220.